Mem. S.A.It. Vol. 77, 429

Memorie della

Fourier-Doppler imaging of non-radial pulsations in γ Doradus stars

S. Jankov[1,2] and P. Mathias[1]

[1] Observatoire de la Côte d'Azur, Dpt. Gemini, UMR 6203, F-06304 Nice Cedex 04
[2] Laboratoire Univ. d'Astroph. de Nice (LUAN), UMR 6525, Parc Valrose, F-06108 Nice Cedex 02 e-mail: Slobodan.Jankov@obs-azur.fr

Abstract. This paper deals with a class of non-radial pulsators along the main sequence, namely the γ Doradus stars for which much effort is currently made in order to constrain their pulsation characteristics. However, because of their relatively low amplitude (few tens of mmag in photometry) and due to the long time scales of the variation (between 0.3 and 3 days), the detection and identification of their pulsations is rather difficult, using the photometric data only. Consequently, the spectroscopic studies of the stars having well-known photometric properties are very valuable and we study in detail the line profile variability (LPV) in γ Doradus candidates observed at Observatoire de Haute-Provence during a two-year high-resolution spectroscopy campaign. The non-radial behavior of selected stars is revealed with the advent of Doppler Mapping and two-dimensional Fourier-Doppler Imaging methods for line-profile analysis, which allowed us to detect and identify the pulsation modes described below.

Key words. Line: profiles – Stars: variables: γ Doradus – Stars: oscillations

1. Introduction

The γ Doradus stars are a recently discovered class of periodically variable stars and up to now there were just a few attempts to identify the pulsational modes in them. From line profile variations in γ Doradus itself and using the method of moments to identify the modes of pulsation of the three periodic components, Balona et al. (1996) deduced the (ℓ,m) values: (3,3) for 1.32098 d^{-1}, (1,1) for 1.36354 d^{-1} and (1,1) for 1.47447 d^{-1} frequencies. For two frequencies (0.346 and 0.795 d^{-1}) detected in 9 Aurigae by Krisciunas et al. (1995), using moment method, Aerts & Krisciunas (1996) found that they are manifestation of $\ell = 3$, $|m| = 1$ spheroidal mode and its toroidal corrections due to the rotation of the star. For two of four frequencies observed in HD 164615, Zerbi et al. (1997) suggested a $\ell = 3$ mode (1.2328 and 0.1301 d^{-1}), while the other two frequencies were associated to $\ell = 2$ (1.0899 d^{-1}) and $\ell = 1$ (2.3501 d^{-1}) modes. Considering a single periodic variation (1.2321 d^{-1}) in the star, Hatzes (1998) found the $|m| = 2$ mode to be consistent with the amplitude of the radial velocity variations. A preliminary mode identification based on the observed color curves of HD 218396 from a multisite campaign (Zerbi et al. 1999) indicated $\ell = 2$ (1.9791 d^{-1}), $\ell = 1$ (1.7268 d^{-1}) and either a $\ell = 1$ or $\ell = 2$ for

Send offprint requests to: S. Jankov

$1.6498\,\mathrm{d}^{-1}$ frequency. For the period 2.67 days in HD 207223, Aerts & Kaye (2001) found a $\ell = m = +2$ solution. Recently, Handler et al. (2002) determined the $\ell = |m| = 1$ value for two observed γ Doradus type non-radial pulsations (with frequencies 0.85 and $1.06\,\mathrm{d}^{-1}$) in the A-type primary of the eccentric binary HD 209295. Applying the method of Dupret et al. (2003) to the lightcurves of HD 12901 and HD 48501, Aerts et al. (2004) found that only an $\ell = 1$ mode was able to explain the observed ratios for the three frequencies for the two stars for all wavelengths. Using the Fourier-Doppler Mapping technique (see next section) Mathias et al. (2004b) determined an $\ell = 3 - 4$ for the $1.94\,\mathrm{d}^{-1}$ frequency in HD 218396.

2. Doppler Mapping of Non-Radial Pulsations

The non-radial pulsator model describes the surface intensity distribution and velocity field perturbations in terms of the associated Legendre functions $P_\ell^m(b, \phi_\mathrm{R})$ and time t as:

$$A_\mathrm{I} P_\ell^m(\sin b) e^{i(m\phi_\mathrm{R} + \omega t)}, \tag{1}$$

where A_I is the oscillation amplitude, $\omega = 2\pi f$ is the angular time frequency in the observer's frame, the quantum numbers (ℓ, m) denote the pulsation degree and azimuthal order, respectively, b is the latitude and ϕ_R is the azimuth related to the rotational frequency of the star Ω_R. The rotational phase should be related to the NRP wave frequency Ω_W defined as:

$$m\Omega_\mathrm{W} t = m\phi = m\phi_\mathrm{R} + \omega t,$$

where ϕ is the corresponding azimuth defined by the same relation.

In rapid rotators, there is a one-to-one mapping between the points in the broadened line profile and the position of perturbations on the stellar surface (Vogt & Penrod (1983)). The technique of the so-called "Doppler mapping" led to various methods to identify pulsation parameters (degree ℓ and order m) from high-resolution, high signal-to-noise spectroscopic observations. Since for the sectoral modes ($|m| = \ell$) most of the variability is located at the equator of the star, and for tesseral modes ($|m| \neq \ell$) the main source of variability lies off the equator, the determination of b is closely related to the modal analysis.

The photospheric absorption line in which rotation is the dominant broadening mechanism displays time-variable perturbations ("bumps" or "deeps") which are carried (as the star rotates) across the stellar disk, causing the bumps to change their Doppler shifts in accordance with their projected distances from the stellar rotation axis which depends on azimuth ϕ:

$$\Delta\lambda = \frac{\lambda}{\mathrm{c}}\, V_\mathrm{e} \sin i\, \cos b\, \sin\phi, \tag{2}$$

where the projected rotational velocity $V_\mathrm{e} \sin i$ is known, for example from Fourier analysis of the average profile as shown in Fig. 1. Relating the azimuth to time t through: $\phi = \frac{\omega}{m}\, t$, the "bump" paths, corresponding to the observed frequency f, can be traced in the dynamic (wavelength/time) spectrum. In addition, the NRP phase Φ can be measured by fitting the sinusoids in each wavelength bin of the dynamic spectrum. The phase diagrams (wavelength/Φ) can be used to determine b, relating ϕ (in Eq. 2) to Φ through: $\phi = \frac{\Phi}{m}\, 2\pi$. From the above equations it is obvious that the "bump" paths, as well as NRP phases, trace out a sinusoidal variation with an amplitude equal to $V_\mathrm{e} \sin i\, \cos b$, from which b can be deduced if $V_\mathrm{e} \sin i$ is known. This value of b depends also on m, and should be consistent with ℓ that can be evaluated using other methods (e.g. Fourier-Doppler Imaging). The latter approach leads to the two-dimensional Fourier analysis in both time and space and its main advantage is that it decomposes complex line profile variations represented as a sum of terms in Eq. 1 into the single components. The wavelength is mapped onto stellar longitude ϕ using:

$$\phi_i = \sin^{-1}\!\left(\frac{c}{\lambda}\frac{\Delta\lambda_i}{V_\mathrm{e} \sin i}\frac{1}{\cos b}\right) \tag{3}$$

where $\Delta\lambda_i$ is the Doppler shift with respect to the line center, corresponding to the wavelength bin i.

Generally, when tesseral modes are present, the corresponding normalized wavelength frequency more closely represents the

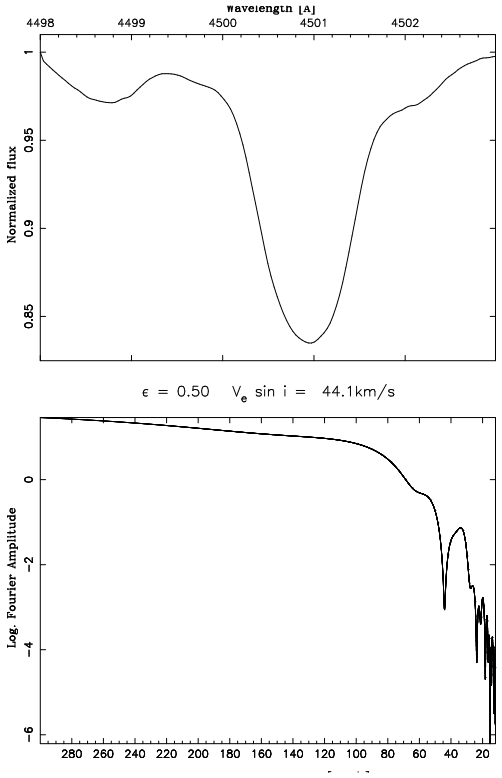

Fig. 1. The average spectrum of Ti II line (top) and its Fourier transform (bottom). The first minimum of the Fourier transform points toward the projected rotational velocity of the star.

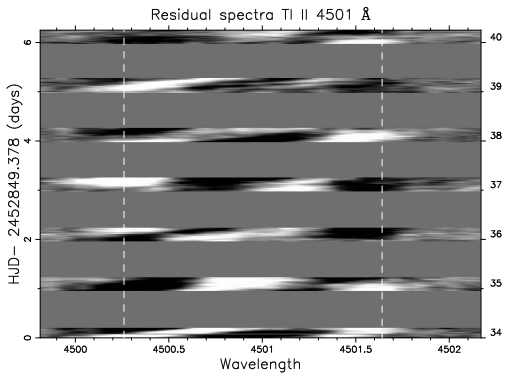

Fig. 2. Dynamic residual spectra (average spectrum subtracted) of 7 nights of the data of the Ti II 4501 Å line. Vertical lines indicate the wavelengths corresponding to the projected rotational velocity.

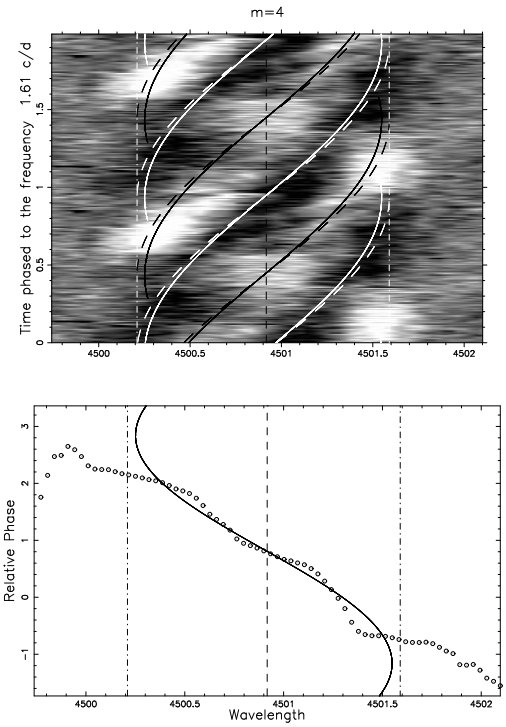

Fig. 3. Top-: dynamic spectrum of residuals folded with the frequency 1.61 d^{-1}. $|m| = 4$ mode at $b = 0°$ (dashed) and $b = 20°$ (full). Bottom: NRP phases and sinusoidal fit.

non-radial degree ℓ rather than the azimuthal order m (Kennelly et al. 1996).

3. Application to HD 195068

We present here the application of the method to the spectra gathered from July 28 to August 4, 2003 at the Observatoire de Haute-Provence with the AURELIE spectrograph (Mathias et al. 2004a). We consider the unblended Ti II line at 4501.273 Å for which the average spectrum and its Fourier transform are shown in Fig. 1 at the top and bottom respectively.

In Fig. 2, gray-scale representations of the time series of the residual spectra with respect to the average profile, obtained during the 7 consecutive nights are shown. In addition to previously detected photometric frequencies, time series analysis performed on this data

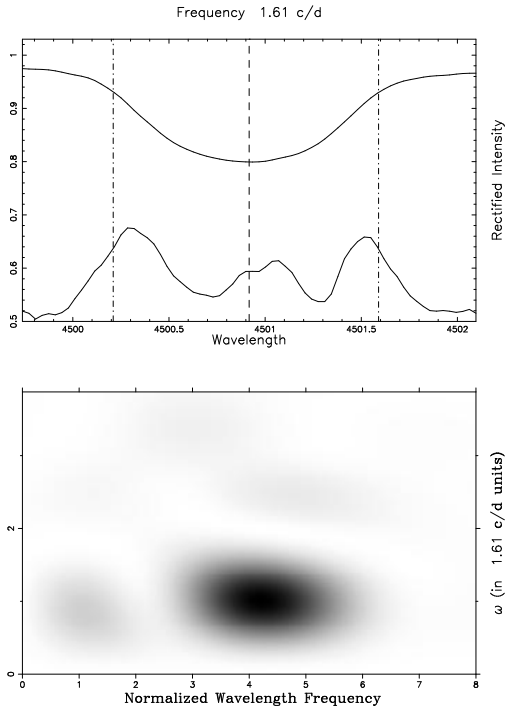

Fig. 4. Top: NRP amplitudes and average profile. Bottom: Fourier-Doppler Image.

(Jankov et al. 2005) shows a main peak at $1.61\,\mathrm{d}^{-1}$. Although the star pulsation is multi-periodic and complex, the line-profile variabilities caused by the individual pulsation modes are separated in frequency as a result of the Fourier analysis which allows the characteristics of this mode to be studied separately. The dynamic spectrum of residuals (average spectrum subtracted) folded with $1.61\,\mathrm{d}^{-1}$is presented in the Fig. 3 (top) where the "bump" paths correspond to a $|m| = 4$ mode confined to the equator (dashed lines) or to the latitude $b = 20°$ (full lines). In the bottom panel the measured NRP phases are plotted as circles, while the full line represents the sinusoidal fit which corresponds to $b = 20°$. The measured NRP amplitudes across the line profile as presented at the top of the Fig. 4 indicate a significant tangential velocity component of oscillations characteristic of high radial order gravity modes, while the Fourier-Doppler diagram plotted at the bottom reveals a $\ell \sim 5 \pm 1$ mode.

4. Conclusions

The application of Fourier-Doppler Imaging technique, reveals an intermediate degree ($\ell \approx 4$) non-radial pulsation modes in HD 195068 (this study) as well as in HD 218396 (Mathias et al. 2004b). The previous photometrically determined low degree ($\ell = 1 - 3$) modes in other γ Doradus stars could be than just a consequence of the observational selection since the spectroscopy is much more sensitive to the intermediate and high degree non-radial pulsation modes.

References

Aerts, C., Krisciunas, K., 1996, MNRAS, 278, 877
Aerts, C., Kaye, A. B., 2001 ApJ, 553, 814
Aerts, C., Cuypers, J., De Cat, P., Dupret, M. A., et al., 2004, A&A, 415, 1079
Balona, L. A., Bohm, T., Foing, B. H., Ghosh, K. K., et al., 1996 MNRAS, 281, 1315
Dupret, M.-A., De Ridder, J., De Cat, P., Aerts, C., et al., 2003, A&A, 398, 677
Handler, G., Balona, L. A., Shobbrook, R. R., Koen, C., et al., 2002, MNRAS, 333, 262
Hatzes, A. P., 1998, MNRAS, 299, 403
Jankov, S., Mathias, P., Chapellier, E., Le Contel, J.-M., Sareyan, J.-P., 2005, submitted to A&A.
Kennelly, E.J., Walker, G.A.H., Catala, C., Foing, B.H., et al., 1996, A&A, 313, 571
Krisciunas, K., Griffin, R. F., Guinan, E. F., Luedeke, K. D., McCook, G. P., 1995, MNRAS, 273, 662
Mathias, P., Le Contel, J.-M., Chapellier, E., Jankov, S., et al., 2004a, A&A, 417, 189
Mathias, P., Chapellier, E., Le Contel, J.-M., Jankov, S., et al., 2004b, ESA SP-538, Second Eddington Workshop, 9 - 11 April 2003, Palermo, Italy, F. Favata, S. Aigrain and A. Wilson. eds., p.355
Vogt, S.S., Penrod, G.D., 1983, PASP, 95, 565
Zerbi, F. M., Rodríguez, E., Garrido, R., Martín, S., et al., 1997, MNRAS, 292, 43
Zerbi, F. M., Rodríguez, E., Garrido, R., Martín, S., et al., 1999, MNRAS, 303, 275